Position-space renormalisation group for isolated polymer chains

1981 J. Phys. A: Math. Gen. 14 2679

(http://iopscience.iop.org/0305-4470/14/10/022)

J. Phys. A: Math. Gen. **14** (1981) 2679–2703. Printed in Great Britain

Position-space renormalisation group for isolated polymer chains†

S Redner and P J Reynolds‡

Center for Polymer Studies§ and Department of Physics, Boston University, Boston, Mass., USA, 02215

Received 12 January 1981, in final form 30 March 1981

Abstract. We develop a cell position-space renormalisation group (PSRG) with which we study the scaling properties of isolated polymer chains. We model a chain by a self-avoiding walk constrained to a lattice. For rescaling factors $b \leqslant 6$, we calculate recursion relations analytically on the square lattice with several different choices for the PSRG weight function. We also calculate implicit cell-to-cell transformations in which a cell of size b is rescaled to a cell of size b'. The results of these PSRGs improve both as b increases and as $b/b' \to 1$. In addition, we construct a true infinitesimal PSRG transformation, which appears to become exact as the dimensionality d approaches 1; we obtain the closed-form expression for the correlation length exponent, $\nu = (d-1)/(d \ln d)$. The Flory formula deviates from this already at first order in $(d-1)$.

We also develop a constant-fugacity Monte Carlo method which enables us to simulate—in an unbiased way within the grand canonical ensemble—chains of up to 10^3 bonds. With this method, we extend the PSRG to larger cells ($b \leqslant 150$) on the square lattice. Our numerical method provides high statistical accuracy for all cell sizes. However, in the range of b we study, the asymptotic behaviour of our results appears to depend on the choice of weight function. One weight function provides smooth behaviour as a function of b, and with it we extrapolate to find $\nu = 0.756 \pm 0.004$. Further work is required to resolve the apparent anomalies in the results based on the other weight functions.

1. Introduction

The properties of a self-avoiding walk (SAW) in the asymptotic 'scaling' limit—when the number of steps N tends to infinity—has been the focus of extensive investigation (see e.g. de Gennes (1979) and references therein). Much of the motivation for these studies comes from an attempt to understand the statistical behaviour of long chain polymers, which may be modelled by SAWs. One of the most direct scaling properties of a polymer is the dependence of the mean end-to-end length on the number of monomers N in the chain. For large N, it is found that

$$\xi(N) \equiv \langle R^2(N) \rangle^{1/2} \sim aN^{\nu}, \tag{1.1}$$

where a is a constant of the order of the lattice spacing, and ν is the exponent describing

† A preliminary account of this work was given at the 43rd Statistical Mechanics Meeting at Rutgers University in May 1980, and a fuller account was presented at STATPHYS 14, Edmonton, Alberta, Canada in August 1980.

‡ Also at NRCC, Lawrence Berkeley Laboratory, Berkeley, CA, USA, 94720.

§ Supported in part by grants from AFOSR and ARO.

the power law divergence of this length. As a first approximation, one may neglect the excluded-volume interaction of the polymer chain, and obtain $\nu = \frac{1}{2}$ for all spatial dimensions d. In a better approximation, Flory (1953) was able to account for the excluded volume by a mean-field-like approach. This gives, when generalised to arbitrary dimensionality d (Fisher 1969),

$$\nu = 3/(d+2). \tag{1.2}$$

This remarkably simple formula—valid for $1 \leqslant d \leqslant 4$—is exact for both $d = 1$ and $d = 4$, and appears to be a very accurate approximation in $d = 2$ and 3. However, it disagrees with the ε expansion for $d = 4 - \varepsilon$, already at first order in ε (de Gennes 1972). Furthermore, as we shall show in § 4, it does not agree with an ε expansion in $1 + \varepsilon$ dimensions either.

Subsequent to Flory's theory, there was considerable numerical work, both in $d = 2$ and $d = 3$, to estimate the various critical exponents of the polymer problem. During this period, the Flory formula for ν was thought to be exact, and the close agreement of the numerical estimates with equation (1.2) added further support to this belief. McKenzie (1976) gives an extensive review of these results. However, des Cloizeaux (1976) pointed out that the physical arguments leading to the Flory formula are not correct. This has led to renewed interest in obtaining accurate estimates for ν in order to test the Flory theory quantitatively. For example, Le Guillou and Zinn-Justin (1977) have applied field theory to a continuum SAW model in $d = 3$, and obtain $\nu = 0.588 \pm 0.001$. Their work was the first to claim that the Flory value of $\nu = 0.6$ in $d = 3$ is incorrect. Recently, Cotton (1980) has re-analysed data from several recent experiments and obtains $\nu = 0.586 \pm 0.004$. Baumgartner (1980) has also presented evidence to confirm the 'non-classical' value of ν for the continuum model, by a Monte Carlo renormalisation group based on decimating along the chemical sequence (de Gennes 1972). However, more extensive work based on this method now gives error bars for ν which include the Flory value (Kremer *et al* 1981). Thus, in three dimensions, it appears that ν may be less than 0.6, although the issue does not seem completely resolved.

On the other hand, a similar effort to obtain ν accurately in two dimensions is just beginning. There have been some position-space renormalisation group (PSRG) studies of a qualitative nature, which employ simpler methods than those used in three dimensions. Shapiro (1978) was the first to apply a decimation procedure directly on the SAW configurations; while this method was a very useful conceptual advance, it is not very accurate numerically. Napiórkowski *et al* (1979) considered a cell PSRG using the Niemeijer–van Leeuwen (1976) approach. From a second-order cumulant approximation requiring five parameters, they obtained $\nu = 0.712$ and 0.769, on the square and triangular lattices respectively. Kremer *et al* (1981) find $\nu = 0.74 \pm 0.01$ based on an extensive study using the Monte Carlo renormalisation method introduced by Baumgartner (1980). de Queiroz and Chaves (1980) have developed a cell PSRG based on the PSRG of Reynolds *et al* (1977) for percolation. For the small cell sizes they considered (involving rescaling factors $b = 2$, 3, 4), their results for the critical parameters improved systematically as b increased. They extrapolated their results to obtain $\nu \cong 0.72$–0.73. In three dimensions, however, the necessary systematic improvement at small b does not occur (Family 1981), indicating that such extrapolations from a few points may be quite risky. Nevertheless this extrapolation idea is very appealing. It has been successfully applied for both the Ising model (Friedman and

Felsteiner 1977) and for percolation (Reynolds *et al* 1978, 1980). These extrapolations, however, require data over a fairly extensive range of b to achieve their accuracy. Very recently, Derrida (1981) has also applied extrapolation ideas to a 'phenomenological' renormalisation procedure on a square lattice with periodic boundary conditions, from which he claims that $\nu = 0.7503 \pm 0.0002$. However, in our opinion, the non-monotonicity of his results with free boundary conditions raises questions about systematic errors in his extrapolation. We discuss these questions with respect to our work in §7. Overall in $d = 2$, however, there appears to be no consensus on the value of ν; any deviation from the Flory value—if one exists—appears to be quite small.

In this paper we develop a cell PSRG for an isolated polymer chain, which we then extend to large cells. Our approach therefore has the potential for the systematic improvement and the accuracy inherent in the large-cell technique. In § 2, we develop the basic ideas of our procedure. Although our basic method is similar to that of de Queiroz and Chaves (1980), we go substantially beyond their work by systematically considering many different weight functions, and by generalising the PSRG to large cells. In § 3 we define several physically plausible weight functions for the square lattice, and we discuss the nature of the approximations associated with them. With these weight functions we then calculate closed-form recursion relations for a cell-to-bond transformation with rescaling parameters $b \leqslant 6$. In § 4, the cell-to-bond transformations are used to construct implicit cell-to-cell transformations (Reynolds *et al* 1978) with rescaling lengths b/b'. Our transformations yield progressively more accurate results both as b increases, and as b/b' approaches 1. We also construct a true infinitesimal transformation by analytically continuing the cell-to-bond transformation to $b \to 1$. This procedure gives $p^* = 1/d$, and $\nu = (d-1)/(d \ln d)$. These are reasonable approximations for $d \leqslant 4$, and we believe they may be exact for $d = 1 + \varepsilon$.

In § 5 we develop a Monte Carlo method to simulate a polymer chain at constant fugacity, in order to extend the PSRG to larger cells. Our procedure generates a collection of isolated chains of varying N, chosen in an unbiased fashion from the grand canonical ensemble. In this way we are able to study chains on the square lattice with up to 10^3 bonds. Then, in § 6, we apply this method to calculate the recursion relations numerically, with high statistical accuracy, for cells of linear size up to $b = 150$. In § 7 we discuss the extrapolation of our $b \leqslant 150$ results to $b \to \infty$. However, the extrapolation for ν appears to depend on the choice of weight function defining the RG rule, at least in the range of b accessible in our study. We discuss several possible sources of this effect. One weight function, on a toroidal cell, appears to extrapolate smoothly to the asymptotic limit; from it we obtain $\nu = 0.756 \pm 0.004$. Finally, in the appendices we present our closed-form recursion relations.

2. Cell position-space renormalisation group

To perform a PSRG calculation on a polymer chain, we study how the characteristic quantities describing a SAW change upon repeated length rescaling of the system. When these quantities remain invariant, the chain is 'self-similar' on all length scales, and this is a 'fixed point' of the rescaling transformation. The invariance of the correlation length, ξ, at such a point implies that $\xi = 0$ or ∞, and the latter fixed point corresponds to criticality.

To carry out the length rescaling, we begin by dividing the lattice into cells which both cover the lattice and preserve the lattice symmetry. On the square lattice we

choose the $b \times b$ *bond* cell of the form shown on the top of figure 1(*a*) (Reynolds *et al* 1977). Upon rescaling the lattice by a factor of b, each cell maps into two bonds, as shown on the bottom of the figure. In principle, an infinite number of parameters are required to describe exactly the chain and its behaviour under rescaling. It is clearly not possible to deal with this infinite parameter space, and somewhere there must be a truncation. We study an approximation in which we deal with only one parameter, a fugacity per monomer p, and we attempt to improve upon the accuracy inherent in this approximation by increasing the cell size.

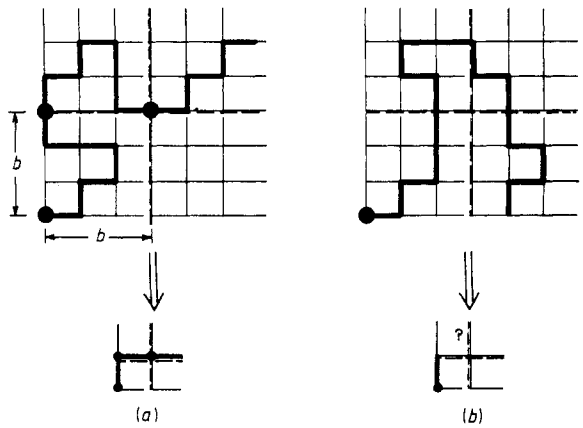

Figure 1. (*a*) Four $b \times b$ cells on the square lattice which rescale to four '1×1' cells. We show a segment of a typical SAW and its rescaled counterpart using the corner rule. This SAW must enter and leave each cell at a corner (heavy dot). (*b*) Another SAW, which is not properly rescaled with the corner rule. A more general weight function is required to handle this walk.

A basic step in this renormalisation procedure is choosing which polymer configurations should contribute to a renormalised bond. The formulation of this rule defines the weight function of the PSRG. In the truncated parameter space we choose, each choice of weight function results in a somewhat different approximation. In the next section we propose several possible weight functions, and discuss the properties and results associated with each. In every case, we map a single SAW within a cell into a rescaled bond if the walk traverses the cell—i.e. gets from one edge to the opposite edge of the cell.

For a given choice of weight function, we calculate the recursion relation as follows. The fugacity per monomer, p, results in a statistical weight p^N for an N-step SAW. The sum of the weights over all traversing configurations defines a grand partition function (Shapiro 1978, de Queiroz and Chaves 1980, Redner and Reynolds 1981),

$$\mathscr{Z}(p) = \sum_N a_N p^N, \tag{2.1a}$$

where a_N is the total number of N-step SAWs that traverse the cell. We impose the condition that this partition function is the same on the original and rescaled levels. Thus

$$\mathscr{Z}'(p') = \mathscr{Z}(p). \tag{2.1b}$$

Hence we obtain a relationship between p and the rescaled fugacity p'. If we rescale to a cell with $b = 1$, then $\mathscr{Z}'(p')$ is simply p', and the recursion relation has the form

$$p' = \sum_N a_N p^N. \tag{2.1c}$$

Equation (2.1c) has two trivial, stable fixed points at $p^* = 0, \infty$; these $\xi = 0$ fixed points correspond respectively to no chain present, and to a densely packed chain that visits every site of the lattice. In addition to these, for every weight function we have studied there is also one unstable fixed point. This fixed point corresponds to a system with $\xi = \infty$—a polymer chain at criticality. The value p^* is the fugacity at which the associated weight for a traversing chain is itself p^*—and there exists on average only one of these. Thus at p^* (and for N sufficiently large), on average an N-step SAW spawns just *one* $(N+1)$-step SAW. In this situation (the fugacity of the next step) × (the average number of choices for the next step) = 1. The 'average number of choices for the next step' is just the effective lattice coordination number μ; hence $\mu = 1/p^*$.

To obtain the exponent ν of equation (1.1), we note that $\xi(p) \equiv \langle R^2(p)\rangle^{1/2} \sim (p - p_c)^{-\nu}$. Thus (Niemeijer and van Leeuwen 1976)

$$\nu = \ln b / \ln \lambda_p, \tag{2.2a}$$

where the eigenvalue λ_p is given by

$$\lambda_p \equiv \mathrm{d}p'/\mathrm{d}p|_{p^*}. \tag{2.2b}$$

Thus far, our discussion has been for general b. For the smallest cell ($b = 2$), however, the PSRG calculations require minimal effort. The results of such calculations (de Queiroz and Chaves 1980, Family 1980) give reasonably good estimates for p^* and ν (see table 1). This is a very desirable feature of the small-cell PSRG approach.

In principle, one can obtain improved accuracy by using a larger *cluster* of cells, and appropriately enlarging the parameter space to include additional fugacities for longer-range links joining further-neighbour monomers (see e.g. Napiórkowski *et al* 1979). These additional parameters are required to maintain the proper *intercell* correlations upon rescaling. This approach is undesirable because the number of parameters quickly becomes very large. To improve the accuracy of the small-cell calculation, but still maintain the simplicity of the one-parameter approach, we will consider larger *cells*. This idea was applied to the Ising model by Friedman and Felsteiner (1977), who used Monte Carlo techniques to calculate the recursion relation for a two-cell cluster. For $b \leqslant 15$, they found that the estimates for the critical exponents systematically improved for increasing b. Similarly, Reynolds *et al* (1978, 1980) developed a cell PSRG for percolation, in which they treated $b \leqslant 500$. The extrapolation of these finite-cell results yields estimates for critical parameters which are of somewhat greater accuracy than those of series expansions and direct MC simulations. Moreover, Reynolds *et al* (1980) give a heuristic argument that the errors due to the approximation in the PSRG for percolation should vanish in the large-cell limit.

In our current approach for the polymer chain, we account for the configurations within the cell to a good approximation, but treat the connection of chains between cells only very approximately. While it seems that this should introduce an error proportional to the surface-to-volume ratio of the cell, it is not clear that this is literally the case. Nevertheless the results of our closed-form PSRG with small cells indicate a trend

Table 1. Results of the small-cell PSRG for the various weight functions. '2-cell' and '3-cell' refer to clusters of two and three adjacent cells. The best known value for p^* is $p^* = 0.000\,015$ (Sykes *et al* 1972).

b		2	3	4	5	6
Corner	p^*	0.4656†	0.4468†	0.4348†	0.4264	0.4202
	ν	0.7153†	0.7187†	0.7217†	0.7241	0.7258
Corner	p^*	0.4656	0.4422	0.4294		
2-cell	ν	0.7153	0.7225	0.7260		
Corner	p^*	0.4656	0.4406			
3-cell	ν	0.7153	0.7241			
Centre	p^*		0.4253		0.4072	
	ν		0.7450		0.7514	
Equal	p^*	0.4656	0.4394	0.4251	0.4161	0.4100
averaging	ν	0.7153	0.7283	0.7352	0.7393	0.7421
T-matrix	p^*	0.4656	0.4385	0.4240	0.4149	0.4088
	ν	0.7153	0.7303	0.7377	0.7421	0.7449
T-matrix	p^*	0.4656	0.4380	0.4231		
2-cell	ν	0.7153	0.7288	0.7355		
T-matrix	p^*	0.4656	0.4378			
3-cell	ν	0.7153	0.7283			
Torus	p^*	0.3660	0.3707	0.3725	0.3734	
	ν	0.6897	0.7050	0.7122	0.7165	

† Also obtained by de Queiroz and Chaves (1980), but their results for $b = 4$ are in error in the third decimal place.

toward the 'correct' asymptotic limit. Therefore one of our interests is to test whether a large-cell PSRG for polymer chains continues this desirable behaviour, thereby permitting accurate estimates of critical exponents.

3. Closed-form recursion relations for small cells

In this section, we present the various rules (weight functions) we have used for specifying a traversing SAW. These rules reflect the possible ways that one might intuitively define 'getting across' a cell. Each rule has qualitatively different characteristics, and we discuss the nature of the associated approximations and results. The recursion relations discussed in this section may be obtained from the appendices.

3.1. Corner rule

To make contact with other work, we first consider the weight function which is used by de Queiroz and Chaves (1980) and Family (1980), and then extend their results. We fix the starting point of the SAW to be a corner (e.g. lower-left) of the cell. Walks which leave the cell via the right edge rescale to a horizontal step, whereas walks leaving by the top edge rescale to a vertical step.

We note that the results obtained from rescaling the 2×2 cell ($b = 2$) are quite good for the amount of effort required, and the results improve for larger b. The recursion relations for $b = 3$ are still relatively simple to calculate by hand, but for $b > 3$ these calculations are prohibitively time-consuming. We have therefore written a computer program to enumerate all traversing walks, and thus extend our closed-form PSRG calculation to $b = 6$. Our results are summarised in the first line of table 1.

We obtain reasonable estimates for the critical parameters. Moreover, the dependence of these parameters on b is such that a rough visual extrapolation to $b \to \infty$ (see e.g. figure 4) yields estimates for p^* and ν which are even closer to their best known values.

3.2. Centre rule

In this rule, we fix the starting point of the SAW to be in the middle of one cell edge (restricting ourselves to cells in which b is odd). Only those SAWs which reach the opposite edge of the cell are counted as traversing. For a given cell size, the results for this rule give an even better approximation to the values of p_c and ν than the corner rule (fourth line of table 1).

3.3. Multiple cells and equal averaging

The above two weight functions nevertheless impose several rather significant approximations on the one-parameter PSRG. First, the starting point of the SAW is fixed in the cell. Thus, it is very unlikely that a traversing SAW in one cell will terminate at the starting point for a SAW in the next cell. Second, there exist certain configurations—e.g. walks which leave the cell either by the same edge or the edge adjacent to the one by which the walk entered—which can contribute to an infinitely long chain, but which do not traverse according to the corner or centre rules. Therefore particular classes of SAWs cannot be properly rescaled within this approximation (see figure 1(b)).

To estimate the magnitude of these approximations, we treat multiple-cell clusters by the corner rule. We renormalise a cluster of two neighbouring $b \times b$ cells into a two-step walk if a SAW traverses both cells. The 'mismatching' of two traversing SAWs across adjacent $b \times b$ cells may be estimated from the difference between the results of the one-cell and two-cell clusters. Comparing these two results, we see that both p^* and ν change by small but significant amounts (second line of table 1). A three-cell cluster also shows this behaviour (third line of table 1). Thus it appears that properly interconnecting walks between cells may be important for obtaining the correct critical exponents.

To avoid the arbitrariness associated with fixing the starting point, and the resulting problem of connecting SAWs between cells, we average over the possible starting points of the SAW (line 5 of table 1). However, because the starting points are not equivalent, a transfer-matrix formalism appears to be a more natural procedure. (A similar transfer-matrix formalism has also been used in the context of 'phenomenological' renormalisation by Derrida (1981).)

3.4. Transfer matrix

We calculate the statistical weight $T_{ij}(p)$ for all SAWs which start at the ith position at one edge of the cell, and exit at the jth position at the opposite edge (see figure 2). These

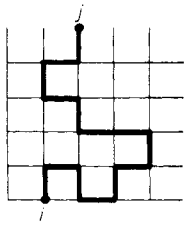

Figure 2. A typical traversing SAW which contributes to the ijth element of the T-matrix recursion relation.

partial contributions to $\mathscr{Z}(p)$ define the $b \times b$ transfer matrix, $T(p)$. The largest eigenvalue of this matrix (a polynomial in p) is a recursion relation reflecting a weighted average over all possible starting points, such that the same relative weight is present at the far edge of the cell. Pictorially, the T-matrix corresponds to starting the SAW in the 'current' cell at the point where the SAW in the 'previous' cell has terminated, and repeating this process for an ensemble of SAWs. As b increases, the T-matrix eigenvector at p^* differs increasingly from the vector, $(1, 1, \ldots, 1)$, which would lead to equal averaging. There is a corresponding increase in the difference of the estimates for ν by the two methods. The results are shown in line 6 of table 1.

Although the T-matrix explicitly addresses the problem introduced by the arbitrariness in the choice of the origin, this procedure is less readily extended to large cells than the other rules. A simpler procedure is to wrap the cell onto a torus. Such a cell is translationally invariant, and *all* starting points are equivalent.

3.5. Toroidal cell

Our weight function on the torus renormalises all SAWs which attain a winding number of ± 1 with respect to the (arbitrary) starting point of the chain (see figure 3). This may be achieved in four independent ways; hence $\mathscr{Z}'(p') = 4p'$. Since there are more traversing configurations here than on our cells with free boundaries, we are able to calculate closed-form recursion relations only for $b \leq 5$. We note that at given b, estimates for p^* are better, but estimates for ν are worse than those from the rules treated above. However, extrapolation of the toroidal small-cell results to $b \to \infty$ yields estimates fairly consistent with those from the other rules (see figure 4).

The translational invariance of the toroidal cell removes the problem of interconnecting walks between cells. This construction also enables us to treat a larger class of walks than we could before. In terms of a block rescaling picture, however, a toroidal cell amounts to allowing various blocks to 'slide' (see figure 5). This sliding leads to

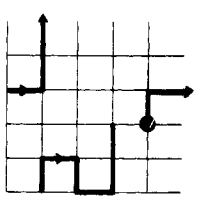

Figure 3. A traversing SAW on a toroidal cell, which has wound once around the torus vertically with respect to the arbitrary starting point which is indicated by the heavy dot.

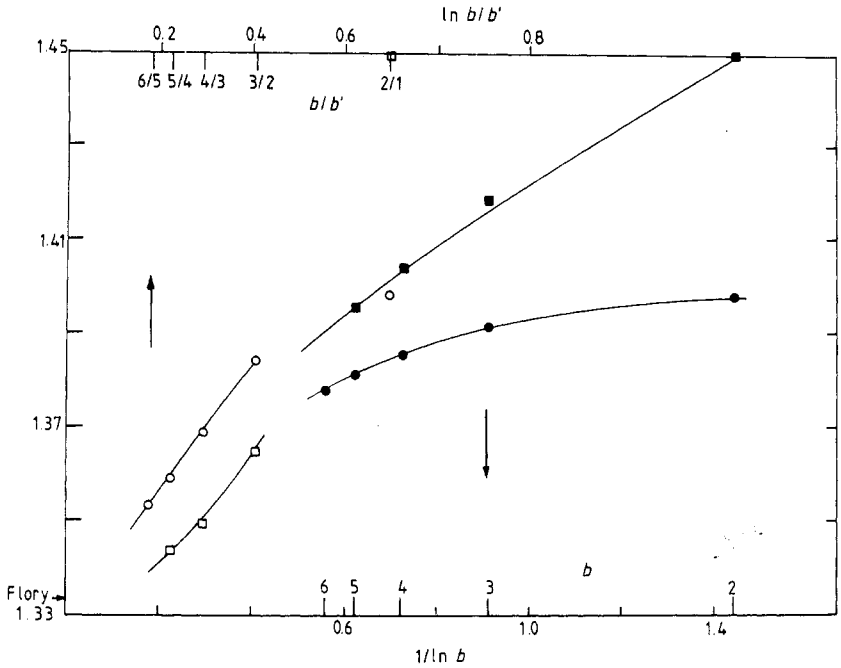

Figure 4. Plots of $y_p(b)$ against $1/\ln b$ for closed-form cell-to-bond transformations (lower horizontal scales), and plots of $y_p(b/b')$ against $\ln b/b'$ for cell-to-cell transformations (upper horizontal scales), for the corner and toroidal weight functions. Cell-to-bond: ■ torus, ● corner; cell-to-cell: □ torus, ○ corner.

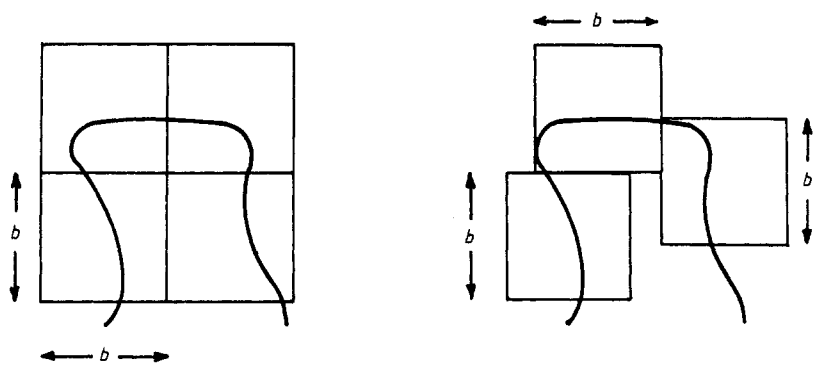

Figure 5. 'Sliding' of toroidal cells in the block rescaling picture. The toroidal cells may be thought of as blocks that slide, so that a chain (shown schematically) must traverse a distance b within each cell. This treats a larger class of SAWs than we could with free boundary conditions. However, there is a new approximation: cells no longer cover the lattice, and they can overlap.

approximations of an entirely different nature from those introduced by the previous rules. For example, different blocks may now overlap.

To summarise, for cells with free boundaries there are two primary approximations: (1) properly interconnecting traversing walks between cells, and (2) properly treating

other configurations which do *not* traverse, but contribute to an infinite walk nonetheless. The toroidal cell partially alleviates these problems, but only at the expense of introducing new approximations. The sliding cells no longer cover the lattice, and cells can overlap. We shall return to these points in § 7, where we find that in extending the PSRG to larger cells the approximation used can strongly influence the numerical results.

4. Cell-to-cell and infinitesimal transformations

In the process of extending the small-cell PSRG results to *larger* b, we also find transformations for which $b \to 1$ (Wilson and Kogut 1974). One way we do this is with a 'cell-to-cell' transformation (Reynolds *et al* 1978). Through the cell-to-bond transformations described in § 3 above, we have the recursion relations $p'(b) = R(b:p)$. Similarly, for a cell of linear size $b' < b$ the recursion relation is $p'(b') = R(b':p)$. These two relations have inverses, and so we may write an implicit transformation (Reynolds *et al* 1978)

$$p'(b/b') = R[b:R^{-1}(b':p'(b'))] \equiv R(b/b':p'(b')). \tag{4.1}$$

This relation gives the total statistical weight for a walk to traverse a cell of size b as a function of the statistical weight for a walk to traverse a cell of size b'. From equation (4.1), the correlation length exponent is

$$\nu = \ln(b/b')/\ln[\lambda_p(b)/\lambda_p(b')], \tag{4.2}$$

where $\lambda_p(b)$ is the eigenvalue of the usual cell-to-*bond* transformation (with rescaling factor b), evaluated at the fixed point of the cell-to-*cell* transformation.

Typical results of this transformation are shown in table 2. The results improve if either b/b' increases, or $b/b' \to 1$. In fact, the accuracy of the cell-to-cell transformation for $b/b' = \frac{6}{5}$ is comparable to the usual cell-to-bond transformation ($b' = 1$) with $b \sim 40$–80. Although it would be worthwhile to extend the cell-to-cell transformation with MC to smaller b/b', the statistical accuracy of our procedure is not sufficient to give results superior to the large-cell PSRG to be discussed in §§ 6 and 7.

However, we can calculate the cell-to-bond recursion relation in the limit $b \to 1$ *analytically*, yielding a true infinitesimal transformation (Shapiro 1978, 1980). To obtain this limit, we construct upper and lower bounds on the cell-to-bond recursion relation for general rescaling factor b and spatial dimension d. In the limit $b \to 1$, the two bounds become identical, thereby yielding the infinitesimal transformation. To construct a lower bound, for example, it is easy to see that there is at least one N-step SAW which traverses a cell of linear size b for $b \leqslant N \leqslant b^d$. Thus we define

$$p'_{\text{lower}} = \sum_{N=b}^{b^d} p^N = (p^b - p^{b^d+1})/(1-p). \tag{4.3a}$$

The upper bound for p', on the other hand, depends on the weight function, although for all our weight functions p'_{upper} approaches the *same* limit as $b \to 1$. Consider, for example, the corner rule. The first few terms in the exact recursion relation include 1 walk of b steps, b walks of $b+1$ steps, and b^2 walks of $b+2$ steps. For longer walks, the self-avoiding constraint ensures that the number of N-step traversing SAWs does not continue this exponential growth. Thus an upper bound for the recursion relation is

$$p'_{\text{upper}} = \sum_{N=b}^{b^d} b^{N-b} p^N = (p^b - b^{b^d-b+1} p^{b^d+1})/(1-p). \tag{4.3b}$$

Table 2. Results of the cell-to-cell transformations for (*a*) the corner rule and (*b*) the toroidal rule.

(*a*) Corner rule.

b	b'	1	2	3	4	5
2	p^*	0.4656				
	ν	0.7153				
3	p^*	0.4468	0.4319			
	ν	0.7187	0.7224			
4	p^*	0.4348	0.4234	0.4160		
	ν	0.7217	0.7260	0.7307		
5	p^*	0.4264	0.4173	0.4112	0.4068	
	ν	0.7241	0.7285	0.7330	0.7360	
6	p^*	0.4202	0.4126	0.4075	0.4038	0.4011
	ν	0.7258	0.7303	0.7346	0.7373	0.7389

(*b*) Toroidal rule.

b	b'	1	2	3	4
2	p^*	0.3660			
	ν	0.6897			
3	p^*	0.3707	0.3747		
	ν	0.7050	0.7329		
4	p^*	0.3725	0.3751	0.3754	
	ν	0.7122	0.7363	0.7412	
5	p^*	0.3734	0.3754	0.3757	0.3759
	ν	0.7165	0.7383	0.7425	0.7443

Letting $b \to 1$, these bounds both become

$$p' = p + (b-1)(1-pd)p \ln p/(1-p). \tag{4.4}$$

In addition to $p^* = 0, \infty$, we find a fixed point at

$$p^* = 1/d, \tag{4.5a}$$

with

$$\nu = (d-1)/(d \ln d). \tag{4.5b}$$

The results for p^* and ν are quite reasonable. We obtain $\nu = 1.0$, 0.721, 0.607 and 0.541 for $d = 1$, 2, 3 and 4 respectively. This transformation is certainly not exact, probably containing the same approximations inherent in the finite-cell approach. However, this infinitesimal transformation exhibits a character similar to the Migdal–Kadanoff transformation (Shapiro 1978) which is exact as $d \to 1$. Thus we believe that

equations (4.5) may become exact as $d \to 1$. For $d = 1 + \varepsilon$, the infinitesimal transformation yields, to $\mathcal{O}(\varepsilon)$, $\nu = 1 - \varepsilon/2$. The Flory formula, in contrast, gives $\nu = 1 - \varepsilon/3$. Thus, just as in $d = 4 - \varepsilon$ (de Gennes 1972), the Flory formula appears to give too large a value for ν.

5. Constant-fugacity Monte Carlo method

To continue on our primary course—extending our PSRG to large cells—we need another method to calculate the recursion relations. This is because the time required to calculate the coefficients a_N in equation (2.1) increases as $\exp(b^d)$. However, knowledge of the a_N (i.e. the full recursion relation) is not necessary. We need information only in the vicinity of the critical fugacity, p^*. To this end, in this section we develop a MC method to simulate a single chain at constant fugacity.

To begin, we note that the recursion relation, equation (2.1*c*), is a generating function for traversing SAWs. More generally, we may consider the generating function for *all* SAWs starting at the origin of an infinite lattice,

$$\Gamma(p) = \sum_N c_N p^N, \tag{5.1a}$$

where c_N is the number of all SAWs of N steps.

In our MC procedure we calculate the value of the generating function at fugacity p by an exact enumeration process. We first construct, with a weight p, each one-step walk that fits on the lattice. We then add the next step to the existing SAWs also with a weight p. Repeating this procedure, we build an ensemble of walks with an associated weight (probability if $p < 1$) p^N for each N-step walk. This process of building walks is quite similar to the methods employed by series to calculate c_N, although series are generally limited to $N < N_{\max} \cong 20$, since

$$c_N \sim \mu^N N^{\gamma - 1} \tag{5.1b}$$

grows exponentially in N. Our weighting factor of p^N helps balance this growth so that we are not forced to restrict ourselves to $N < N_{\max}$. Instead, we generate a subset of all isolated chains, in which N fluctuates and the polydispersion is controlled by the statistics of the grand canonical ensemble.

For p less than the critical value $p_c = 1/\mu$, the total weight, $c_N p^N$, of all N-step walks in the ensemble decreases exponentially with N (cf equation 5.1(*b*)). Thus the mean length of the SAWs in the ensemble is finite. At p_c, the product of p_c times the mean number of possible next steps μ, is unity. The number of walks now grows slowly—only as a power law in N—and walks of *all* length scales are represented. Above p_c, the number of N-step walks grows exponentially with N. Thus the dominant contribution to any configurational property comes from the longer walks. In the limit $p \to \infty$, these properties are determined by the longest possible SAWs only—i.e. those which visit every site in the lattice. These walks correspond to a completely ordered, zero-temperature phase (Redner and Reynolds 1981).

Our numerical technique has several advantages over conventional MC methods. For example, on the square lattice, we are able to sample chains of approximately 10^3 bonds, free from any systematic bias, with only moderate use of computer time (1.73 hours on an IBM 370/168 for 10^5 complete enumerations at p^* for the periodic 150×150 square lattice). On the other hand, the conventional first-principle MC

simulations (see e.g. Wall *et al* (1963) and references therein) can only sample chains of length approximately 10^2 on the square lattice. With considerable technical refinement (see e.g. Wall *et al* 1963, Alexandrowicz 1968), longer chains can be sampled, but only at the expense of introducing some systematic bias. Various dynamical MC methods have also been developed to study a single polymer chain (see e.g. Verdier and Stockmayer 1962, Wall and Mandel 1975, Lax and Brender 1977), but these methods also introduce statistical bias, depending on the dynamic processes chosen to allow the chain to evolve (Hilhorst and Deutsch 1975). Even the latest work we are aware of (Kremer *et al* 1981) simulated chains with $N \leqslant 10^2$, though in a continuum.

In addition, we calculate configurational properties in terms of a temperature-like variable, p, rather than in terms of N. This permits us to probe directly chain properties both above and below the phase transition. For example, we can find the mean end-to-end distance through

$$\xi^2(p) = \sum_{N,r} r^2 c_{N,r} p^N \Big/ \sum_{N,r} c_{N,r} p^N \sim (p - p_c)^{-2\nu} \tag{5.2}$$

where $c_{N,r}$ is the number of N-step SAWs starting at the origin and terminating at a point a distance r away. (This type of measurement is appropriate for the region $p < p_c$ where $\xi(p)$ is finite.)

We are, however, primarily interested in the regime $p \cong p_c$, to study the scaling behaviour of a polymer chain. To complete a simulation of the generating function in a finite amount of time, we use a finite lattice. For $p = p_c$, a characteristic length scale is then imposed by the linear size b of the system. This is the basis of finite-size scaling (Fisher 1971, Sur *et al* 1976, Reynolds *et al* 1978). These arguments lead to (see also Redner and Reynolds 1981)

$$\langle N[p_c(b)] \rangle \sim b^{1/\nu}, \tag{5.3}$$

where $\langle N[p_c(b)] \rangle$ is the average number of steps in the ensemble of SAWs at criticality.

When we return to the PSRG in the next section, we will be interested in the generating function for *traversing* SAWs rather than the generating function for *all* SAWs. This difference requires only minor modifications in applying the MC procedure given above. Moreover, we will see that there is a close relation between $\langle N[p_c(b)] \rangle$ for traversing SAWs and the eigenvalue of the renormalisation group transformation. This result enables us to connect the PSRG with finite-size scaling, and aids us in the extrapolation of our large-cell results to $b \to \infty$.

6. Monte Carlo recursion relations for large cells

Using the constant-fugacity MC method described in the previous section, we may evaluate the recursion relation at any given value of p. We do this by building chains within a $b \times b$ cell, adding each step with a weight p. Thereby we simulate a grand canonical ensemble of traversing SAWs at fugacity p. Through many repetitions of this simulation process, we obtain numerically $p'(p)$ by counting the number of walks which traverse the cell.

To locate the fixed point, p^*, we begin with a zeroth 'guess', p_0, and we make our next estimate, p_1, depending on whether $p'(p_0)$ is greater or less than p_0. A trial and error search must be repeated many times in order to converge accurately to p^*, and this is impractically slow for large cells. In figure 6 we see that for $p < p^*$ (except for a small

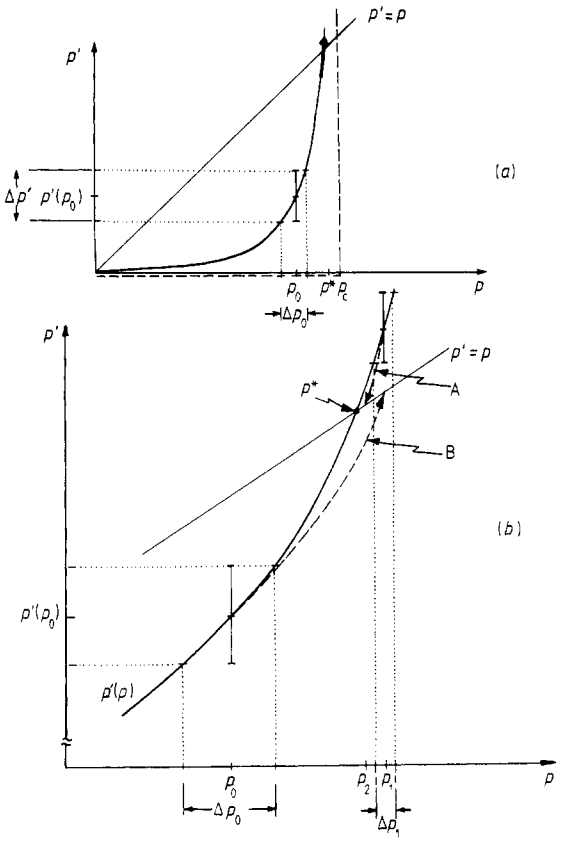

Figure 6. (*a*) Schematic plot of the recursion relation $p'(p)$ for a large cell. This function varies rapidly near p^*, and for $b \to \infty$ it approaches the limiting form: $p'(p) = 0$ for $p < p_c$ (broken line), $p'(p_c) = p_c$, $p'(p) = \infty$ for $p > p_c$. The schematic data point on the curve is derived from measurement of the average number of traversing walks per enumeration at fugacity p_0. The error bar for $p'(p)$ is determined by statistics. We determine an error bar for p by horizontally extending the error bars for $p'(p)$ until they intersect the tangent at $p'(p_0)$. The value of the slope to the curve at p^* (arrow) is the eigenvalue of the recursion relation. (*b*) A magnification of the behaviour near p^* to illustrate the homing procedure. Starting at p_0, we use the MC information to construct a parabolic approximation to the recursion relation. The intercept of this approximation (curve B) with the line $p' = p$ yields p_1. From p_1, we then iterate to p_2 (curve A). We terminate the homing when the uncertainty $\Delta p'(p_i)$ is such that Δp_i includes the next intercept, p_{i+1}.

range of p very close to p^*), very few SAWs survive to traverse the cell, and we gain little information on the location of p^*. On the other hand, for p above p^*, the number of traversing walks is so large that simulations at this fugacity are prohibitively time consuming.

Instead, to locate p^* quickly, we devised a 'homing' procedure that relies on the simple form of the recursion relation equation (2.1). The first and second derivatives of p',

$$dp'/dp = \sum_N N a_N p^{N-1}, \qquad d^2p'/dp^2 = \sum_N N(N-1) a_N p^{N-2}, \qquad (6.1a)$$

are simply related to the averages, $\langle N(p) \rangle$ and $\langle N(p)^2 \rangle$, which we can calculate directly

by our MC method. We find

$$dp'/dp = p'\langle N(p)\rangle/p, \qquad d^2p'/dp^2 = p'(\langle N^2\rangle - \langle N\rangle^2)/p^2. \tag{6.1b}$$

Thus, in addition to finding p' at p_0, we also find p' in a small neighbourhood of p_0:

$$p'(p) = p'(p_0) + (p-p_0)\,dp'/dp|_{p_0} + \tfrac{1}{2}(p-p_0)^2\,d^2p'/dp^2|_{p_0} + \ldots. \tag{6.2}$$

Starting with p_0, we iterate to p_1 by solving equation (6.2) for the value of p at which $p'(p_1) = p_1$. We obtain

$$p = p_0 + \left\{\frac{dp'}{dp} - 1 + \left[\left(\frac{dp'}{dp} - 1\right)^2 + \frac{2d^2p'}{dp^2}(p-p')\right]^{1/2}\right\} \Big/ \frac{d^2p'}{dp^2}. \tag{6.3}$$

Geometrically this solution corresponds to approximating $p'(p)$ at p_0 by the parabola of equation (6.2), and finding the intersection of this curve with the line $p' = p$ (see figure 6(b)).

We repeat this homing process until the difference between the ith guess, p_i, and $p'(p_{i-1})$ is less than the statistical uncertainty in $p'(p_{i-1})$. Typically, our initial estimates for p^* were correct to within two significant figures. The homing process then found p^* to four significant figures with only three to four iterations.

Having found p^*, we determine ν from the eigenvalue of the linearised recursion relation at p^* (cf equation (2.2)). This eigenvalue is simply the first derivative in equation (6.1), evaluated at p^*; this may be directly measured in our MC. However, to calculate this quantity accurately is difficult, because dp'/dp is a rapidly varying function of p, and the statistical errors associated with it are relatively large (see figure 7). From equation (6.1b), we see that the dispersion in λ_p will be the product of the errors for p' and $\langle N(p)\rangle$.

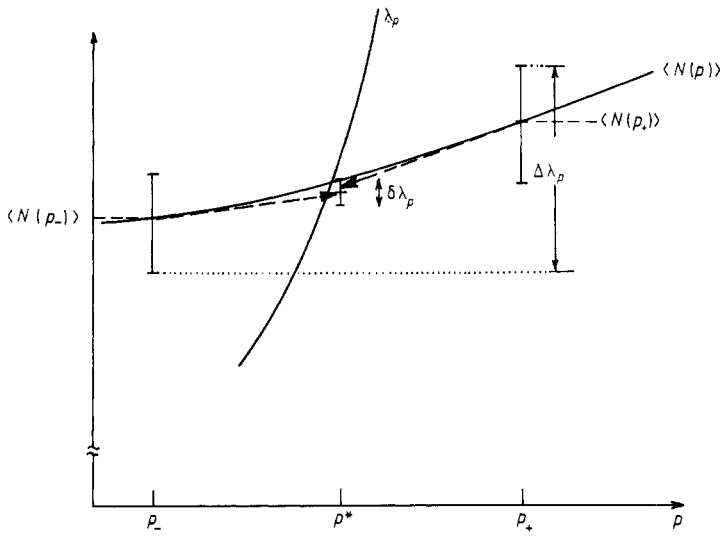

Figure 7. Comparison of λ_p and $\langle N(p)\rangle$ in the vicinity of p^*. We measure $\langle N(p_\pm)\rangle$ with $p_\pm$ chosen very near but distinct from p^*, using the condition that the error bars for $p'_\pm$ exclude p^* (cf figure 6(b)). From the error bars for $\langle N(p_\pm)\rangle$ we determine an error for the eigenvalue as indicated by $\Delta\lambda_p$. We then use a Taylor expansion to extrapolate linearly values of $\langle N(p)\rangle$ to the estimated value of p^*. From the dispersion in these extrapolated values, we reduce the error bar to $\delta\lambda_p$.

On the other hand, we can measure $\langle N(p)\rangle$ with greater precision because it is a more slowly varying function of p. With the same data, our error bar for $\langle N(p)\rangle$ is 4 to 10 times smaller than the error bar for λ_p, depending on the cell examined. Moreover, at the fixed point

$$\lambda_p = \langle N(p^*)\rangle. \tag{6.4}$$

Thus we focus on $\langle N(p)\rangle$ because of its greater statistical accuracy, and its direct connection with the critical exponent.

To determine the errors in λ_p, we must consider both the statistical uncertainty in $\langle N(p)\rangle$, and the errors made in locating p^*. To this end, we calculate $\langle N(p_+)\rangle$ and $\langle N(p_-)\rangle$, with $p_+ > p^*$ and $p_- < p^*$ chosen such that the statistical error in $p'(p_\pm)$ just excludes the possibility that either p_+ or $p_- = p^*$. Clearly, the upper error bar of $\langle N(p_+)\rangle$ and the lower error bar of $\langle N(p_-)\rangle$ are bounds on λ_p (figure 7).

We can reduce these error bars further by using a procedure similar to that in equation (6.2). We deduce $\langle N(p^*)\rangle$ using our best estimate for p^* from the homing procedure, together with $\langle N(p)\rangle$ calculated near p^*. Starting with the Taylor expansion for $\langle N(p^*)\rangle$,

$$\langle N(p^*)\rangle = \langle N(p)\rangle + (p^* - p)\, \mathrm{d}\langle N(p)\rangle/\mathrm{d}p|_p + \ldots, \tag{6.5a}$$

and using the relation of $\mathrm{d}\langle N(p)\rangle/\mathrm{d}p$ to the fluctuations in $\langle N(p)\rangle$,

$$\mathrm{d}\langle N(p)\rangle/\mathrm{d}p = (\langle N(p)^2\rangle - \langle N(p)\rangle^2)/p, \tag{6.5b}$$

we estimate $\langle N(p^*)\rangle$ by combining these expressions. Pictorially this amounts to constructing the tangent to the curve $\langle N(p)\rangle$, and extending it to p^* (figure 7). This approximation to $\langle N(p^*)\rangle$ becomes more accurate as p approaches p^*, and the higher-order terms in equation (6.5a) become negligible. In actuality, we performed most of our runs sufficiently close to p^* so that there was very good internal consistency between the various 'scaled' values of $\langle N(p^*)\rangle$; the internal consistency remained good even when we included preliminary data from simulations relatively far from p^*. Hence we advantageously combine the information from many runs to reduce our error bars on $\lambda_p(b)$ by factors ranging from 2.5 to 12, depending on the quality of the internal consistency. In table 3 we give our estimates for $\lambda_p(b) = \langle N(p^*(b))\rangle$ for the corner, centre and toroidal weight functions.

7. Extrapolation to $b \to \infty$

For any finite cell of linear dimension b, the PSRG is only approximate. However, it appears possible that the error due to our approximations vanishes as $b \to \infty$ (see e.g. Friedman and Felsteiner 1977, Reynolds *et al* 1978, 1980). Thus the extrapolation of the sequence of finite-cell results should be better than the results obtained with the largest cell considered.

To extrapolate the value of $p^*(b)$, we assume finite-size scaling (Fisher 1971, Sur *et al* 1976, Reynolds *et al* 1978, 1980), from which

$$(p^*(b) - p_c) \sim b^{-1/\nu}. \tag{7.1}$$

Table 3. Results of the large-cell PSRG for: (*a*) the corner rule, (*b*) the centre rule and (*c*) the toroidal rule.

(*a*) Corner rule.

b	10	20	40	80	150
No of realisations ($\times 10^6$)	5.0	4.0	2.0	1.0	2.49
p^*	0.406 00 ±0.000 28	0.393 30 ±0.000 09	0.386 13 ±0.000 12	0.382 44 ±0.000 16	0.380 736 ±0.000 080
$\langle N(p^*)\rangle$	23.51 ± 0.01	60.17 ± 0.03	155.8 ± 0.3	407.0 ± 3	984.2 ± 6
ν	0.729 26 ±0.000 14	0.731 16 ±0.000 09	0.730 72 ±0.000 50	0.729 28 ±0.001 50	0.727 04 ±0.001 10

(*b*) Centre rule.

b	11	21	41	81
No of realisations ($\times 10^6$)	2.90	0.80	1.20	1.45
p^*	0.391 69 ±0.000 26	0.385 37 ±0.000 21	0.382 13 ±0.000 10	0.380 45 ±0.000 06
$\langle N(p^*)\rangle$	23.80 ± 0.01	59.66 ± 0.01	135.1 ± 0.4	334.4 ± 3
ν	0.756 51 ±0.000 12	0.757 48 ±0.000 03	0.756 94 ±0.000 51	0.756 05 ±0.000 22

(*c*) Toroidal rule.

b	10	20	40	80	150
No of realisations ($\times 10^6$)	3.52	2.95	1.20	1.50	1.35
p^*	0.375 56 ±0.000 33	0.376 82 ±0.000 16	0.377 85 ±0.000 08	0.378 37 ±0.000 13	0.378 705 ±0.000 060
$\langle N(p^*)\rangle$	23.87 ± 0.01	59.95 ± 0.03	150.2 ± 0.3	373.0 ± 2	859.0 ± 4
ν	0.725 77 ±0.000 11	0.731 82 ±0.000 08	0.736 01 ±0.000 29	0.740 01 ±0.000 70	0.741 68 ±0.000 51

For the three rules studied in the large-cell limit—corner, centre and toroidal—we have plotted our data of $p^*(b)$ against b^{-1/ν_t}, with a trial value of $\nu_t = \frac{3}{4}$ (figure 8). According to equation (7.1), the points should fall asymptotically on a straight line with intercept p_c at $b^{-1/\nu_t} = 0$. Extrapolation of the sequences $p^*(b)$ for all three rules gives almost identical results. We estimate $p_c = 0.3791 \pm 0.0001$ on the square lattice, consistent with but not as accurate as the result $p_c = 0.379\,003 \pm 0.000\,015$ of Sykes *et al* (1972).

Next we extrapolate the scaling power y_p defined by

$$y_p \equiv \log \lambda_p / \log b = \nu^{-1}. \tag{7.2a}$$

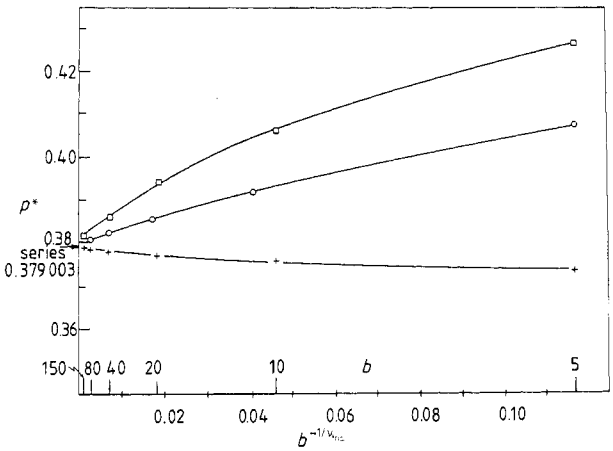

Figure 8. Plot of $p^*(b)$ against $b^{-1/\nu_{\text{trial}}}$ for the corner (□), centre (○) and toroidal (+) rules. In general, the errors in $p^*(b)$ become progressively smaller for larger b, because the increasing steepness of the recursion relation allows us to find the fixed point more precisely. For the data shown, the error bars are smaller than the plotted points. Here $\nu_{\text{trial}} = \frac{3}{4}$. The plots for the centre rule are at $b = 5$, 11, 21, 41 and 81.

There is a difficulty, however, because both the corner and centre rules yield sequences of $y_p(b)$ that are non-monotonic in b, and thus extrapolation is not possible—at least not without additional values of $y_p(b)$ for still larger b. One possibility is that the non-monotonicity is from errors arising in approximations in the PSRG which persist asymptotically in the large-cell limit. Another possibility is that the results will in fact be correct asymptotically. Addressing the first possibility, one important approximation—identified in § 3—is related to the fact that although we take into account walks within the cell to a good approximation, connections between cells are not treated as accurately. To quantify this 'interfacing' problem, we note that the probability that a traversing walk terminates at a particular lattice site is proportional to $1/b^{d-1}$. Therefore, if the starting point of the SAW is fixed, the probability that traversing SAWs in adjacent, independent cells join varies as $1/b^{2d-2}$. Hence the interfacing appears to become worse in the large-cell limit.

However, we may test the asymptotic validity of the cell PSRG through an alternative and simpler approach by employing scaling arguments. If $\langle N(p^*)\rangle \sim b^{1/\nu}$ as $b \to \infty$ as expected from finite-size scaling, then the PSRG should work asymptotically, since this value of ν found by scaling is precisely the same ν as in the PSRG (since $\langle N(p^*)\rangle = \lambda_p$). The centre rule PSRG 'sees' a segment of a polymer chain of length b, confined within a strip of width b; the corner rule sees the SAW as a polymer confined to a wedge-shaped region with opening angle $\pi/4$, with one end of the chain at the apex of the wedge. Such confined polymer systems may be described by the scaling approach of Daoud and de Gennes (1977) and de Gennes (1979). This approach indicates that the confining geometries do not affect the critical behaviour as $b \to \infty$, but rather both systems exhibit the behaviour of a polymer chain in the bulk—$\langle N(p^*)\rangle \sim b^{1/\nu}$. Thus both the corner and centre rule PSRGs *should* yield the correct ν asymptotically. Apparently much larger values of b are still required with these rules. We are currently extending the transfer-matrix approach to large cells. This approach treats the interfacing much better, and we hope that the results based on this method will converge more rapidly.

On the toroidal cell, however, our data for $y_p(b)$ *is* monotonic and very smoothly behaved (see table 3 and figure 9). This supports the importance of interfacing properly, since the toroidal weight function does this better than the corner or centre rules. Extrapolating data for $y_p(b)$ now appears reasonable. We include a quadratic term in the extrapolation to help account for the curvature in the data over the whole range of b. Such a procedure, which neglects terms of $\mathcal{O}[1/(\ln b)^3]$, has been very successful in percolation (Eschbach *et al* 1981, Reynolds 1980, Blöte *et al* 1981). We write

$$y_p(b) = y_p(b=\infty) + C_1/\ln b + C_2/(\ln b)^2 + \ldots, \tag{7.2b}$$

where the constants C_i represent the errors in $y_p(b)$ due to the finite-cell approximation. Equation (7.2b) suggests that we extrapolate the sequence $y_p(b)$ against $1/\ln b$.

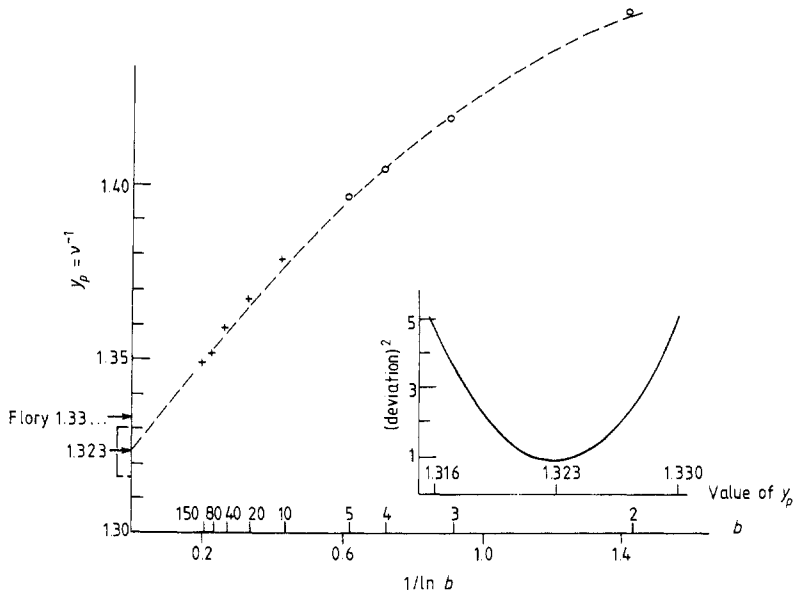

Figure 9. Plot of our estimates of $y_p(b)$ against $1/\ln b$ for the toroidal cell. The open circles are exact data, while the crosses are the Monte Carlo data; the errors are smaller than the size of the plotted points. The broken curve is the best quadratic fit to our data: $y = 1.323 + 0.138x - 0.035x^2$, where $x = 1/\ln b$. The inset shows the squared deviations of the quadratic fit as a function of the intercept. From this, we determine an error of 0.005 for y_p. Including statistical sources of error yields a total error of 0.007 for y_p indicated by the square bracket on the left edge of the figure.

Asymptotically this should be a straight line with intercept $y_p(b=\infty)$. We perform a least-squares fit of $y_p(b)$ to a parabola whose intercept (at $1/\ln b = 0$) is constrained to be y_p^{test}. The minimum of the summed squares of the deviations between the data and the fit (cf inset, figure 9) provides an estimate for the scaling power, y_p^{true}; the sharpness of the parabola gives an indication of the quality of the fit. As a conservative estimate, we choose error bars on y_p by the points at which the summed squared deviations are *three* times larger than at their minimum. Our analysis thus yields $\nu = 0.756 \pm 0.003$.

To estimate the effect of the statistical error in the individual data points, we choose trial values $y_p^{\text{gauss}}(b)$ from gaussian distributions centred at each measured value of

$y_p(b)$, with standard deviations equal to the dispersion of the particular data points (cf table 3). We extrapolate the trial data set using the parabolic least-squares fit described above, and obtain an intercept $y_p^{\text{gauss}}(\infty)$. This extrapolation of gaussian sampled data points is repeated to obtain a distribution of intercepts. The width of this distribution is 0.001, giving an estimate of the probable error in y_p due to the statistical uncertainties in the individual data points. Again being conservative, we add the two sources of error—the estimated systematic error and the statistical error—to yield a total uncertainty of ± 0.004. Actually, the statistical error of each data point is negligible, and it is the systematic error that one must be concerned with. Thus, within the approximation of a toroidal cell PSRG for $b \leq 150$, we estimate that $\nu = 0.756 \pm 0.004$. The Flory value $\nu = 0.75$ seems unlikely from the trend in our data (see figure 9). However, in the light of the non-monotonicity found with the other PSRG weight functions, we cannot exclude the possibility that the Flory value of ν is correct.

8. Concluding remarks

We have developed and implemented a cell PSRG to study the scaling behaviour of a single polymer chain described by a lattice SAW. This PSRG is simple to execute in principle, and yields good approximations for the critical parameters of the SAW problem at the small-cell level. We have investigated ways in which we can improve upon this approximation. One direction is through cell-to-cell and infinitesimal transformations, in which the rescaling factor $b \to 1$. The cell-to-cell method seems to be very accurate, but we can only extend the results to rescaling factor $\frac{6}{5}$. In addition, we have derived a true infinitesimal transformation which gives the analytic expression $\nu = (d-1)/(d \ln d)$. For $d = 1+\varepsilon$, we believe that this PSRG may be exact; in this limit we find $\nu = 1 - \varepsilon/2$, disagreeing with $\nu = 1 - \varepsilon/3$ for the Flory formula.

We have also considered the opposite extreme—the large-cell limit—where the rescaling factor $b \to \infty$. To calculate the recursion relations, we needed first to develop a new MC method, which simulates a grand canonical ensemble of single SAWs at constant fugacity. With this method, we were able to simulate chains of length up to 10^3 on the square lattice efficiently. In contrast, conventional simulations are limited to $N \sim 10^2$ on the square lattice, and considerable technical refinements—which are not entirely free of statistical bias—are required to achieve larger N.

In the large-cell limit we have found that our results were dependent on the weight function. We have argued that a good weight function must treat the 'interfacing' of SAWs between cells adequately. Based on an approximation using a toroidal cell, we estimate that $\nu = 0.756 \pm 0.004$. This value appears to exclude $\nu = 0.75$ predicted by Flory. However, more work is still necessary to settle the value of ν in $d = 2$ definitively.

Acknowledgments

We are grateful to A Coniglio, F Family, L Kadanoff, W Klein, S Muto, H Nakanishi, P Pincus, H E Stanley and D Stauffer for valuable discussions. We also thank D Stauffer for helpful correspondence and comments on the manuscript. In addition, we thank the Boston University Academic Computing Center for providing us with computer time for this project. One of us (SR) thanks the Boston University Graduate School of Science for partial support of this work.

Appendix 1. Elements of the transfer-matrix recursion relations

The transfer-matrix elements given here may be used to obtain all the non-toroidal recursion relations discussed in the text. For example, for the corner rule, $p'(p) = \sum_{j=1}^{b} T_{1j}$.

2 × 2 cell

$$T_{11}(p) = T_{22}(p) = p^2 + p^4$$
$$T_{12}(p) = 2p^3$$

3 × 3 cell

$$T_{11}(p) = T_{33}(p) = p^3 + 3p^5 + 5p^7 + 2p^9$$
$$T_{12}(p) = T_{23}(p) = 3p^4 + 5p^6 + 2p^8$$
$$T_{13}(p) = 6p^5 + 4p^7 + 2p^9$$
$$T_{22}(p) = p^3 + 6p^5 + 2p^7$$

4 × 4 cell

$$T_{11}(p) = T_{44}(p) = p^4 + 6p^6 + 16p^8 + 39p^{10} + 61p^{12} + 47p^{14} + 8p^{16}$$
$$T_{12}(p) = T_{34}(p) = 4p^5 + 14p^7 + 32p^9 + 42p^{11} + 36p^{13} + 13p^{15}$$
$$T_{13}(p) = T_{24}(p) = 10p^6 + 28p^8 + 38p^{10} + 39p^{12} + 27p^{14} + 4p^{16}$$
$$T_{14}(p) = 20p^7 + 36p^9 + 48p^{11} + 48p^{13} + 32p^{15}$$
$$T_{22}(p) = T_{33}(p) = p^4 + 12p^6 + 27p^8 + 29p^{10} + 27p^{12} + 15p^{14} + p^{16}$$
$$T_{23}(p) = 4p^4 + 24p^6 + 28p^8 + 28p^{10} + 22p^{12} + 6p^{14}$$

5 × 5 cell

$$T_{11}(p) = T_{55}(p) = p^5 + 10p^7 + 40p^9 + 125p^{11} + 400p^{13} + 1048p^{15} + 1905p^{17} + 2372p^{19} + 1839p^{21} + 764p^{23} + 86p^{25}$$
$$T_{12}(p) = T_{45}(p) = 5p^6 + 30p^8 + 96p^{10} + 285p^{12} + 693p^{14} + 1269p^{16} + 1741p^{18} + 1619p^{20} + 806p^{22} + 128p^{24}$$
$$T_{13}(p) = T_{35}(p) = 15p^7 + 69p^9 + 211p^{11} + 472p^{13} + 857p^{15} + 1276p^{17} + 1457p^{19} + 1046p^{21} + 405p^{23} + 58p^{25}$$
$$T_{14}(p) = T_{25}(p) = 35p^8 + 147p^{10} + 352p^{12} + 679p^{14} + 1143p^{16} + 1645p^{18} + 1714p^{20} + 870p^{22} + 143p^{24}$$
$$T_{15}(p) = 70p^9 + 224p^{11} + 510p^{13} + 956p^{15} + 1586p^{17} + 2224p^{19} + 2106p^{21} + 732p^{23} + 104p^{25}$$
$$T_{22}(p) = T_{44}(p) = p^5 + 20p^7 + 75p^9 + 207p^{11} + 452p^{13} + 841p^{15} + 1263p^{17} + 1340p^{19} + 811p^{21} + 188p^{23}$$

$$T_{23}(p) = T_{34}(p) = 5p^6 + 50p^8 + 156p^{10} + 312p^{12} + 564p^{14} + 895p^{16} + 1108p^{18} + 924p^{20} + 418p^{22} + 87p^{24}$$

$$T_{24}(p) = 15p^7 + 104p^9 + 240p^{11} + 458p^{13} + 799p^{15} + 1204p^{17} 1360p^{19} + 894p^{21} + 228p^{23}$$

$$T_{33}(p) = p^5 + 20p^7 + 110p^9 + 220p^{11} + 388p^{13} + 634p^{15} + 858p^{17} + 868p^{19} + 570p^{21} + 208p^{23} + 38p^{25}$$

6 × 6 cell

$$T_{11}(p) = T_{66}(p) = p^6 + 15p^8 + 85p^{10} + 335p^{12} + 1237p^{14} + 4638p^{16} + 15\,860p^{18} + 44\,365p^{20} + 99\,815p^{22} + 181\,995p^{24} + 262\,414p^{26} + 285\,086p^{28} + 218\,011p^{30} + 104\,879p^{32} + 26\,344p^{34} + 1770p^{36}$$

$$T_{12}(p) = T_{56}(p) = 6p^7 + 55p^9 + 240p^{11} + 858p^{13} + 3103p^{15} + 10\,233p^{17} + 28\,261p^{19} + 65\,193p^{21} + 125\,039p^{23} + 193\,588p^{25} + 228\,299p^{27} + 190\,671p^{29} + 101\,648p^{31} + 30\,018p^{33} + 3326p^{35}$$

$$T_{13}(p) = T_{46}(p) = 21p^8 + 145p^{10} + 572p^{12} + 2019p^{14} + 6285p^{16} + 16\,709p^{18} + 38\,714p^{20} + 78\,163p^{22} + 132\,761p^{24} + 179\,884p^{26} + 182\,802p^{28} + 130\,266p^{30} + 59\,746p^{32} + 14\,563p^{34} + 935p^{36}$$

$$T_{14}(p) = T_{36}(p) = 56p^9 + 334p^{11} + 1312p^{13} + 4028p^{15} + 10\,617p^{17} + 25\,074p^{19} + 53\,796p^{21} + 101\,853p^{23} + 160\,100p^{25} + 193\,465p^{27} + 168\,685p^{29} + 97\,246p^{31} + 33\,301p^{33} + 4999p^{35}$$

$$T_{15}(p) = T_{26}(p) = 126p^{10} + 726p^{12} + 2496p^{14} + 6947p^{16} + 17\,248p^{18} + 39\,603p^{20} + 83\,442p^{22} + 153\,620p^{24} + 225\,813p^{26} + 234\,937p^{28} + 159\,526p^{30} + 65\,404p^{32} + 13\,252p^{34} + 590p^{36}$$

$$T_{16}(p) = 252p^{11} + 1200p^{13} + 3904p^{15} + 10\,560p^{17} + 25\,828p^{19} + 58\,712p^{21} + 121\,868p^{23} + 217\,436p^{25} + 300\,380p^{27} + 280\,776p^{29} + 170\,384p^{31} + 61\,336p^{33} + 10\,180p^{35}$$

$$T_{22}(p) = T_{55}(p) = p^6 + 30p^8 + 170p^{10} + 608p^{12} + 2080p^{14} + 6556p^{16} + 17\,952p^{18} + 42\,470p^{20} + 85\,138p^{22} + 140\,140p^{24} + 178\,916p^{26} + 163\,605p^{28} + 96\,883p^{30} + 32\,890p^{32} + 4923p^{34} + 144p^{36}$$

$$T_{23}(p) = T_{45}(p) = 6p^7 + 90p^9 + 404p^{11} + 1373p^{13} + 4019p^{15} + 10\,580p^{17} + 25\,088p^{19} + 52\,482p^{21} + 93\,563p^{23} + 135\,218p^{25} + 148\,122p^{27} + 115\,129p^{29} + 58\,754p^{31} + 16\,741p^{33} + 1718p^{35}$$

$$T_{24}(p) = T_{35}(p) = 21p^8 + 215p^{10} + 889p^{12} + 2605p^{14} + 6771p^{16} + 16\,271p^{18} + 35\,869p^{20} + 70\,218p^{22} + 116\,093p^{24} + 151\,421p^{26} + 143\,761p^{28} + 92\,148p^{30} + 36\,010p^{32} + 6865p^{34} + 292p^{36}$$

$$T_{25}(p) = 56p^9 + 460p^{11} + 1606p^{13} + 4486p^{15} + 11\,292p^{17} + 26\,406p^{19} + 56\,774p^{21} + 107\,670p^{23} + 167\,480p^{25} + 192\,072p^{27} + 145\,730p^{29} + 67\,494p^{31} + 16\,268p^{33} + 1288p^{35}$$

$$T_{33}(p) = T_{44}(p) = p^6 + 30p^8 + 240p^{10} + 900p^{12} + 2481p^{14} + 6267p^{16} + 14\,841p^{18} + 31\,979p^{20} + 60\,519p^{22} + 96\,258p^{24} + 121\,433p^{26} + 114\,449p^{28} + 76\,960p^{30} + 33\,895p^{32} + 7943p^{34} + 459p^{36}$$

$$T_{34}(p) = 6p^7 + 90p^9 + 530p^{11} + 1582p^{13} + 4036p^{15} + 9712p^{17} + 21\,848p^{19} + 44\,338p^{21} + 77\,860p^{23} + 112\,528p^{25} + 125\,330p^{27} + 100\,570p^{29} + 55\,210p^{31} + 18\,000p^{33} + 2428p^{35}$$

Cluster of two adjacent 3 × 3 cells

$$T_{11}(p) = T_{33}(p) = p^6 + 15p^8 + 85p^{10} + 125p^{12} + 113p^{14} + 60p^{16} + 16p^{18}$$

$$T_{12}(p) = T_{23}(p) = 6p^7 + 55p^9 + 114p^{11} + 109p^{13} + 60p^{15} + 16p^{17}$$

$$T_{13}(p) = 21p^8 + 75p^{10} + 129p^{12} + 113p^{14} + 60p^{16} + 16p^{18}$$

$$T_{22}(p) = p^6 + 30p^8 + 100p^{10} + 106p^{12} + 60p^{14} + 16p^{16}$$

Cluster of three adjacent 3 × 3 cells

$$T_{11}(p) = T_{33}(p) = p^9 + 36p^{11} + 456p^{13} + 1638p^{15} + 3175p^{17} + 3833p^{19} + 3178p^{21} + 1816p^{23} + 672p^{25} + 128p^{27}$$

$$T_{12}(p) = T_{23}(p) = 9p^{10} + 204p^{12} + 1120p^{14} + 2591p^{16} + 3444p^{18} + 3018p^{20} + 1784p^{22} + 672p^{24} + 128p^{26}$$

$$T_{13}(p) = 45p^{11} + 428p^{13} + 1673p^{15} + 3160p^{17} + 3834p^{19} + 3178p^{21} + 1816p^{23} + 672p^{25} + 128p^{27}$$

$$T_{22}(p) = p^9 + 72p^{11} + 672p^{13} + 2044p^{15} + 3066p^{17} + 2858p^{19} + 1752p^{21} + 672p^{23} + 128p^{25}$$

Cluster of two adjacent 4 × 4 cells

$$T_{11}(p) = T_{44}(p) = p^8 + 28p^{10} + 280p^{12} + 1694p^{14} + 5286p^{16} + 11\,858p^{18} + 21\,065p^{20} + 30\,594p^{22} + 35\,622p^{24} + 31\,496p^{26} + 19\,118p^{28} + 6051p^{30} + 264p^{32}$$

$$T_{12}(p) = T_{34}(p) = 8p^9 + 140p^{11} + 1043p^{13} + 3654p^{15} + 8579p^{17} + 15\,726p^{19} + 23\,319p^{21} + 27\,630p^{23} + 25\,253p^{25} + 16\,503p^{27} + 6400p^{29} + 801p^{31}$$

$$T_{13}(p) = T_{24}(p) = 36p^{10} + 469p^{12} + 2043p^{14} + 5692p^{16} + 11\,904p^{18} + 19\,817p^{20} + 26\,245p^{22} + 27\,331p^{24} + 21\,450p^{26} + 11\,237p^{28} + 2786p^{30} + 111p^{32}$$

$$T_{14}(p) = 120p^{11} + 826p^{13} + 2978p^{15} + 7866p^{17} + 16\,298p^{19} + 26\,556p^{21} + 34\,190p^{23} + 34\,552p^{25} + 25\,996p^{27} + 12\,236p^{29} + 1878p^{31}$$

$$T_{22}(p) = T_{33}(p) = p^8 + 56p^{10} + 602p^{12} + 2548p^{14} + 6213p^{16} + 11\,620p^{18} + 17\,675p^{20} + 21\,446p^{22} + 20\,194p^{24} + 14\,016p^{26} + 6280p^{28} + 1271p^{30} + 47p^{32}$$

$$T_{23}(p) = 8p^9 + 224p^{11} + 1358p^{13} + 4118p^{15} + 8698p^{17} + 14\,750p^{19} + 20\,098p^{21} + 21\,522p^{23} + 17\,566p^{25} + 10\,038p^{27} + 3232p^{29} + 342p^{31}.$$

Appendix 2. Recursion relations on the toroidal cell

2 × 2 cell

$$p' = p^2 + 4p^3 + 2p^4$$

3 × 3 cell

$$p' = p^3 + 6p^4 + 18p^5 + 18p^6 + 28p^7 + 14p^8 + 14p^9$$

4 × 4 cell

$$p' = p^4 + 8p^5 + 32p^6 + 88p^7 + 134p^8 + 278p^9 + 336p^{10} + 564p^{11} + 594p^{12} + 720p^{13} + 618p^{14} + 402p^{15} + 138p^{16}$$

5 × 5 cell

$$p' = p^5 + 10p^6 + 50p^7 + 170p^8 + 466p^9 + 886p^{10} + 2062p^{11} + 3360p^{12} + 7114p^{13} + 10\,576p^{14} + 19\,908p^{15} + 27\,092p^{16} + 44\,628p^{17} + 53\,190p^{18} + 75\,076p^{19} + 71\,136p^{20} + 78\,108p^{21} + 50\,664p^{22} + 36\,724p^{23} + 11\,980p^{24} + 4164p^{25}.$$

References

Alexandrowicz Z 1968 *J. Chem. Phys.* **51** 561
Baumgartner A 1980 *J. Phys. A: Math. Gen.* **13** L39
Blöte H W J, Nightingale M P and Derrida B 1981 *J. Phys. A: Math. Gen.* **14** L45
des Cloizeaux J 1976 *J. Physique* **31** 715
Cotton J P 1980 *J. Physique* **41** L231
Daoud M and de Gennes P G 1977 *J. Physique* **38** 85
Derrida B 1981 *J. Phys. A: Math. Gen.* **14** L5
Eschbach P D, Stauffer D and Herrmann H J 1981 *Phys. Rev.* B **23** 422
Family F 1980 *J. Phys. A: Math. Gen.* **14** L325
—— 1981 *J. Physique* **42** L137
Fisher M E 1969 *J. Phys. Soc. Japan* **26** Suppl 44
—— 1971 *Critical Phenomena: Enrico Fermi Summer School, Varenna, Italy, Course 51* ed. M S Green (New York: Academic)

Flory P J 1953 *Principles of Polymer Chemistry* (Ithaca, New York: Cornell University Press)
Friedman Z and Felsteiner J 1977 *Phys. Rev.* B **15** 5317
de Gennes P G 1972 *Riv. Nuovo Cimento* **7** 363
—— 1979 *Scaling Concepts in Polymer Physics* (Ithaca, New York: Cornell University Press)
Hilhorst H J and Deutsch J M 1975 *J. Chem. Phys.* **63** 5103
Kremer K, Baumgartner A and Binder K 1981 *Z. Phys.* B **40** 331
Lax M and Brender C 1977 *J. Chem. Phys.* **67** 1785
Le Guillou J C and Zinn-Justin J 1977 *Phys. Rev. Lett.* **39** 95
McKenzie D S 1976 *Phys. Rep.* **27C** 35
Napiórkowski M, Hauge E M and Hemmer P C 1979 *Phys. Lett.* **72A** 193
Niemeijer Th and van Leeuwen J M J 1976 in *Phase Transitions and Critical Phenomena* ed C Domb and M S Green (New York: Academic) vol 6
de Queiroz S L A and Chaves C M 1980 *Z. Phys.* B **40** 99
Redner S and Reynolds P J 1981 *J. Phys. A: Math. Gen.* **14** L55
Reynolds P J 1980 unpublished
Reynolds P J, Klein W and Stanley H E 1977 *J. Phys. C: Solid State Phys.* **10** L167
Reynolds P J, Stanley H E and Klein W 1978 *J. Phys. A: Math. Gen.* **11** L199
—— 1980 *Phys. Rev.* B **21** 1223
Shapiro B 1978 *J. Phys. C: Solid State Phys.* **11** 2829
—— 1980 *J. Phys. C: Solid State Phys.* **13** 3387
Sur A, Lebowitz J L, Marro J, Kalos M L and Kirkpatrick S 1976 *J. Stat. Phys.* **15** 345
Sykes M F, Guttmann A J, Watts M G and Roberts P D 1972 *J. Phys. A: Math. Gen.* **5** 653
Verdier P H and Stockmayer W H 1962 *J. Chem. Phys.* **36** 227
Wall F T and Mandel F 1975 *J. Chem. Phys.* **63** 4592
Wall F T, Windwer S and Gans P J 1963 in *Methods in Computational Physics* (New York: Academic) vol 1 p 217
Wilson K G and Kogut J 1974 *Phys. Rep.* **12C** 75